Biophysical Journal, Volume *110*

Supplemental Information

A Microfluidic Platform for Real-Time Detection and Quantification of Protein-Ligand Interactions

Therese W. Herling, David J. O'Connell, Mikael C. Bauer, Jonas Persson, Ulrich Weininger, Tuomas P.J. Knowles, and Sara Linse

Biophysical Journal

Supporting Material

A Microfluidic Platform for Real-Time Detection and Quantification of Protein-Ligand Interactions

Therese W. Herling,[1] David J. O'Connell,[2] Mikael C. Bauer,[3] Jonas Persson,[3,5] Ulrich Weininger,[4] Tuomas P. J. Knowles,[1,*] and Sara Linse[3,*]

[1]Department of Chemistry, University of Cambridge, Cambridge, United Kingdom; [2]School of Biomolecular and Biomedical Science, University of College Dublin, Dublin, Ireland; [3]Department of Biochemistry and Structural Biology and [4]Department of Biophysical Chemistry, Lund University, Lund, Sweden; and [5]Department of Immunology, Genetics and Pathology, Uppsala University, Uppsala, Sweden.

*Correspondence: tpjk2@cam.ac.uk; sara.linse@biochemistry.lu.se

Supporting Material for: A microfluidic platform for real-time detection and quantification of protein-ligand interactions

T.W. Herling[1], D.J. O'Connell[2], M.C. Bauer[3], J. Persson[3], U. Weininger[4], T.P.J. Knowles[1], S. Linse[3]

[1]Department of Chemistry, University of Cambridge, CB2 1EW Cambridge, UK. [2]School of Biomolecular and Biomedical Science, University College Dublin, Dublin 4, Ireland. [3]Department of Biochemistry and Structural Biology, Lund University, 22100 Lund, Sweden. [4]Department of Biophysical Chemistry, Lund University, 22100 Lund, Sweden.

Expression and purification of calmodulin

Full length human calmodulin was expressed from a modified Pet3a vector ('PetSac' with NdeI and SacI cloning sites) containing a synthetic calmodulin gene. The wild-type gene was built with the codons preferred by *Escherichia coli*(1). The calmodulin gene with mutation S17C was amplified by polymerase chain reaction (PCR) from this vector using primers containing the desired base change in two steps using standard procedures. The PCR product was digested by NdeI and SacI and cloned into the PetSac vector.

Following transformation, the mutant protein was expressed in *E. coli* strain BL21(De3)pLysS star in LB medium and the wild-type protein was purified using heat treatment, anion exchange chromatography, hydrophobic interaction chromatography and gel filtration. The purification started with sonication of cell pellet from 4.5 litre culture in a total of 100 mL 20 mM Tris-HCl, 1 mM $CaCl_2$, 1 mM DTT, 20 mM NaCl, pH 7.5 (buffer A). Two portions of 50 mL were sonicated for 1.5 minutes each using a tip sonicator (1/2 horn, maximum output, duty cycle 50%) in a beaker surrounded by ice-water slurry. The sonicates were centrifuged at 18,000 rcf for 10 minutes at $4^{\circ}\mathrm{C}$ (spin 1). The supernatant was poured into 100 mL boiling buffer A and heated to 85°C to precipitate *E. coli* proteins, followed by rapid cooling (beaker gently swirled in surrounding ice-water slurry) and centrifugation at 18,000 rcf for 10 minutes at $4^{\circ}\mathrm{C}$ (spin 2). The supernatant from spin 2 was pumped onto a 5.4 x 12 cm DEAE cellulose column packed and equilibrated in buffer A. The pellet from spin 1 was sonicated in 40 mL of buffer A, centrifuged (spin 3), heat treated and centrifuged (spin 4) as above. The supernatant from spin 4 was loaded onto the same DEAE cellulose column as above. The column was washed with 200 mL buffer A and eluted by a linear gradient from 20 - 500 mM NaCl in 20 mM Tris-HCl, 1 mM $CaCl_2$, 1 mM DTT, pH 7.5, total gradient volume 1200 mL. 10 mL fractions were collected and examined by agarose gel electrophoresis. Fractions containing calmodulin, total volume 650 mL, were pumped onto a 5.4 x 14 cm phenyl sepharose column equilibrated in 50 mM Tris-HCl, 1 mM $CaCl_2$, 1 mM DTT, 150 mM NaCl, pH 7.5. The column was washed with 300 mL of 50 mM Tris-HCl, 1 mM $CaCl_2$, 1 mM DTT, 150 mM NaCl, pH 7.5, followed by elution with 500 mL 50 mM Tris-HCl, 1 mM EDTA, 1 mM DTT, 150 mM NaCl, pH 7.5. 8 mL fractions were collected and examined by UV absorbance at 280 nm, SDS PAGE and agarose gel electrophoresis. Fractions containing calmodulin were combined and lyophilised, followed by desalting on a 3.4 x 20 cm Sephadex G25 superfine column in water through a zone of decalcified NaCl. This resulted in Ca^{2+}-free (apo) calmodulin, which was also free from the EDTA used to chelate Ca^{2+}. The G25 column was first washed with EDTA, pH 7,5, and then Millipore water. 5 mL of saturated NaCl, pH 7.5 (stored in a plastic flask containing 5 ml Chelex resin in a dialysis bag; the dialysis tubing was boiled four times in Millipore water before filling with Chelex resin equilibrated to pH 7.5) was applied to the column directly before the calmodulin sample was applied. The protein was eluted in water and 3 mL fractions collected in plastic tubes, examined by UV absorbance at 280 nm, and lyophilised. This procedure was repeated three times with a third of the protein being desalted in each repeat. The final yield was 770 mg pure apo-calmodulin-S17C, based on the weight of the lyophilised powder.

The purity at protein level was confirmed by agarose gel electrophoresis in EDTA and in Ca^{2+}, and by SDS-polyacrylamide gel electrophoresis. The absence of EDTA and other small molecules was confirmed by ^{1}H NMR spectroscopy. Titrations in the presence of Quin2 were used to quantify the residual Ca^{2+} concentration in the apo protein sample, and found to be less than 0.04 molar equivalents, which is less than 1% of full saturation.

0006-3495/08/09/2624/12 $2.00 doi: xx.xxxx/biophysj.xxx.xxxxxx

Alexa labelling

Calmodulin-S17C was labeled with the fluorescent dye Alexa546 for ProtoArray screening or with Alexa488 for the microfluidic studies. 10 mg calmodulin was dissolved in 20 mM phosphate buffer with 100 mM NaCl, 1 mM EDTA, 1 mM DTT, pH 7.3, incubated for one hour and DTT removed by gel filtration on a NAP-10 column in 20 mM phosphate buffer with 100 mM NaCl, and 1 mM EDTA, pH 7.3 One molar equivalent of Alexa546 C5-maleimide (Invitrogen, California, US) or with Alexa488 C5-maleimide (Invitrogen, California, US) was added and the labelling mixture was then left to react at room temperature in the dark for one hour. Excess unbound dye was removed by passing the reaction twice through a NAP-10 size exclusion column (washed with 5 mL 1 mM EDTA, pH 7,5, and then 15 mL Millipore water, with water as the eluent and collecting the protein fraction. The labelled protein was immediately divided into aliquots and frozen.

Protein array screen

A protein array screen was performed to probe for potential calmodulin binding partners as described in the main text and methods section. In the analysis, Alexa546 labelled calmodulin binding to immobilised protein spots on these arrays targets were recorded, we used a signal intensity above a cutoff of 200. The calmodulin target proteins identified in this screen are shown in SI Fig. 1 and 2. SI Fig. 1 contains the proteins identified in the presence of free Ca^{2+}. The proteins highlighted in bold font were only identified in the presence of calcium ions.

The proteins targeted by calmodulin in the absence of free Ca^{2+} are listed in SI Fig. 2. Systems that were only above the signal intensity threshold for apo-calmodulin are shown in bold font.

Surface plasmon resonance studies

All SPR experiments were carried out using a Biacore 3000 instrument. S17C calmodulin was immobilised using ligand thiol disulphide exchange coupling, following the procedures recommended by the supplier (GE Healthcare). The dextran matrix of a CM5 chip was activated by injecting 25 μL of a fresh mixture of 0.05 M N-hydroxysuccimide, and 0.2 M 1-ethyl-3-(3-dimethylaminopropyl)carbodiimide. A reactive disulphide group was then introduced on the sensor chip surface by injecting 20 μL of 100 μM 2-(2-pyridinyldithio)ethaneamine, PDEA, 0.1 M sodium borate, pH 8.5. Calmodulin was then immobilised by injecting 100 μL of 10 μg/mL calmodulin S17C in 10 mM HCO_2Na (sodium formate), pH 4.3. Finally, residual PDEA groups were deactivated by injecting 40 μL of 50 mM L-cysteine, 1 M NaCl, 100 mM HCO_2Na, pH 4.3. Blank channels for negative control were prepared by omitting calmodulin in the coupling step, and an additional control channel was prepared by immobilisation of human serum albumin. Binding of targets was surveyed by injecting 150 μL of creatine kinase solutions in 10 mM Tris-HCl, 150 mM KCl, 1 mM $CaCl_2$, 0.005% v/v Tween20, pH 7.5. Dissociation of target protein from calmodulin was followed under buffer flow. The chip was then regenerated by injecting 100 μL of 1 M NaCl, 10 mM glycine, pH 2.5. The flow rate was 10 μL/min throughout the experiment. For an SPR experiment, where the expected K_d is on the order of micromolar, 100 picomoles of material would be required for the immobilisation step (100 μL of 1 μM solution). An additional 10 - 200 picomoles of free protein for injection would be consumed depending on the kinetics of binding and dissociation.

The rate constants were obtained by fitting a single exponential decay to the dissociation data after baseline subtraction, right panels in Fig. 2B and SI Fig. 3, using the response, R, as a function of time, t,

$$R(t) = A\, e^{-k_{\rm off} t}, \tag{1}$$

with the variable parameters being the dissociation rate constant, $k_{\rm off}$, and the amplitude of the signal, A. The association phase data, left panels in Fig. 2B and SI Fig. 3, were analysed by fitting the following function:

$$R(t) = R_{\rm max}\, \frac{c k_{\rm on}}{k_{\rm off} + c\, k_{\rm on}} \left(1 - e^{-(k_{\rm off} + c k_{\rm on})t}\right) R_0, \tag{2}$$

using the $k_{\rm off}$ determined with equation 1 and the protein concentration, c. The variable parameters were: the association rate constant, $k_{\rm on}$; the signal at full saturation of all the immobilised targets, $R_{\rm max}$; and the response resulting from the injection of the protein, R_0. The resulting rates constants were $k_{\rm on} = 7.3 \times 10^2\ {\rm M^{-1}s^{-1}}$, $k_{\rm off} = 2.6 \times 10^{-5}\ {\rm s^{-1}}$ for creatine kinase B in the presence of Ca^{2+}. Relating the rate constants to the equilibrium dissociation constant, K_d, through

$$K_d = \frac{k_{\rm off}}{k_{\rm on}} \tag{3}$$

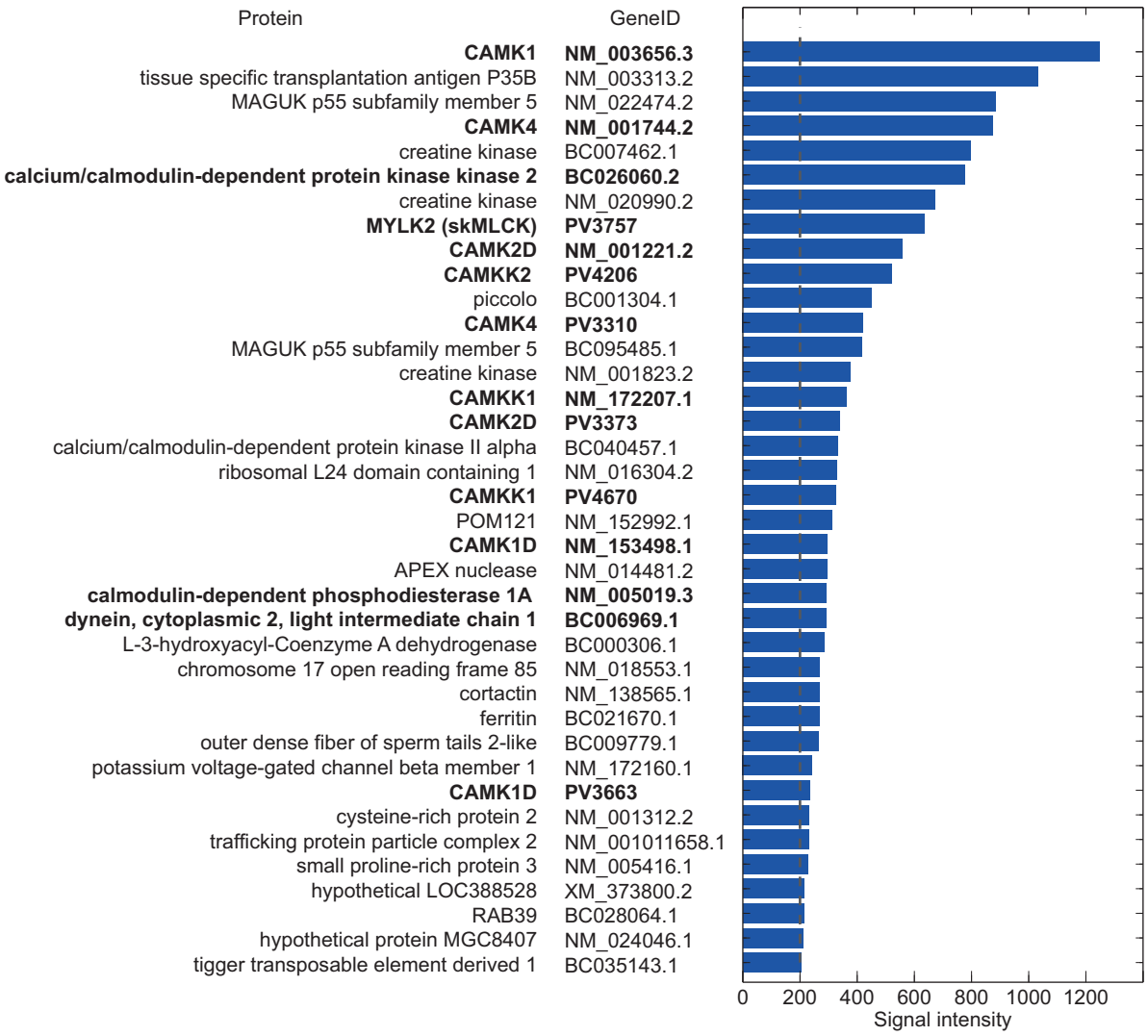

Figure 1: Putative calmodulin targets identified in the ProtoArray screen in the presence of Ca^{2+}. Targets in bold are identified in the presence of Ca^{2+} only.

results in values for the equilibrium dissociation constant of $K_d = 36$ nM for calmodulin binding to creatine kinase B on the sensor chip surface.

Further to the free flow electrophoresis measurements described below, the calcium dependence of the interaction between calmodulin and phosphorylase kinase was also investigated by SPR, SI Fig. 3. In the presence of added Ca^{2+}, rabbit phosphorylase kinase was observed to bind to immobilised calmodulin with a very low dissociation rate. Only limited dissociation was observed over the course of days, as discussed in the main text the slow dissociation of phosphorylase kinase may be due to avidity effects. In the presence of EDTA to chelate any trace Ca^{2+}, we did not observe any binding of phosphorylase kinase to the immobilised calmodulin. The data shown in magenta in SI Fig. 3 has therefore been normalised against the maximum response in the calcium buffer.

In the case of phosphorylase kinase we only observed binding to calmodulin in the presence of Ca^{2+}, SI Fig. 3. Fitting this data as described above resulted in $k_{\mathrm{on}} = 3.1 \times 10^4$ M^{-1} s^{-1} and $k_{\mathrm{off}} = 1 \times 10^{-6}$ s^{-1}. As mentioned in the Discussion section, the very low observed k_{off} could be an artefact due to binding of one multimeric phosphorylase kinase to multiple immobilised copies of calmodulin. In this situation phosphorylase kinase would be required to dissociate simultaneously from up to four copies of calmodulin before leaving the surface of the chip.

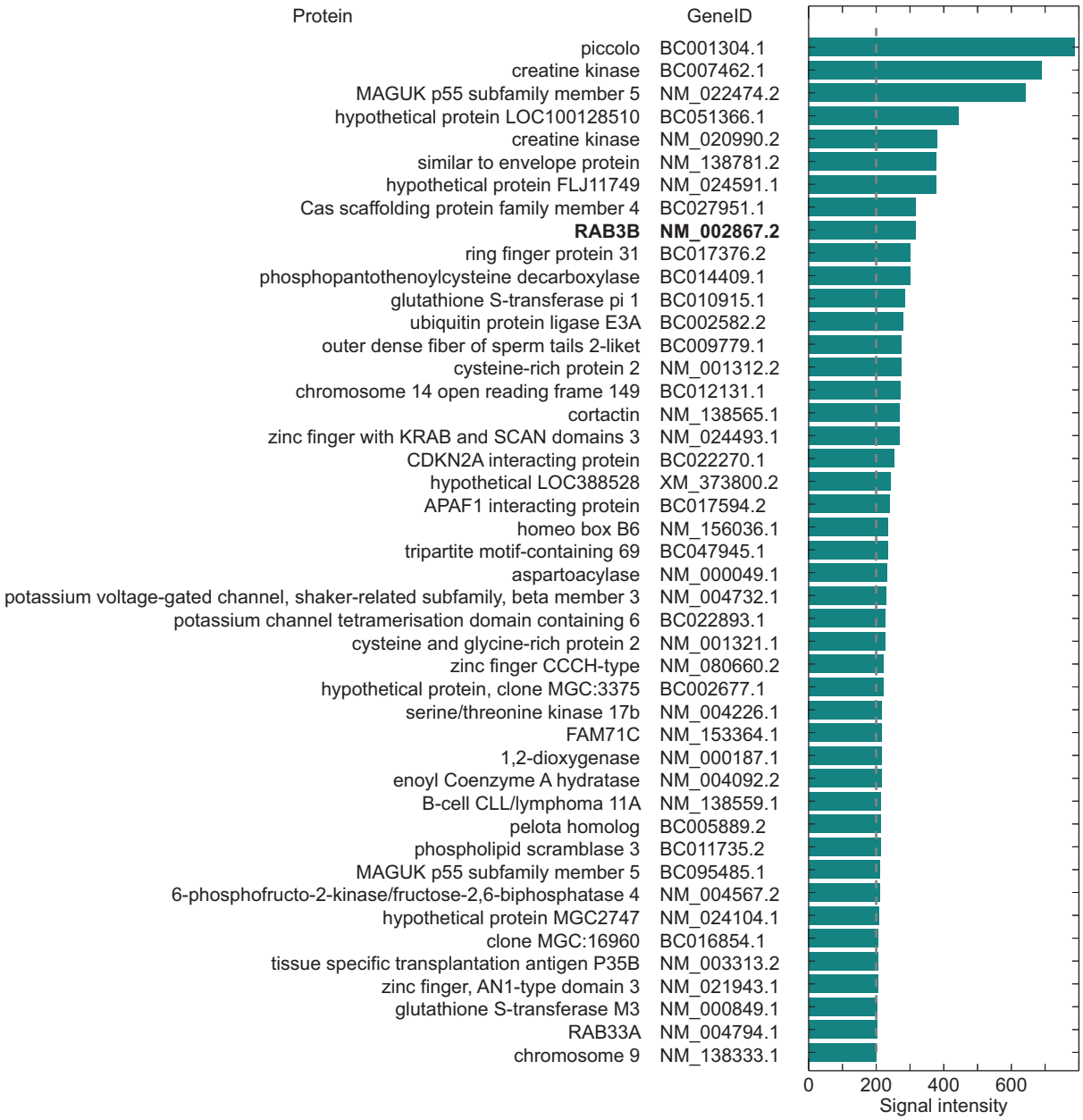

Figure 2: Putative calmodulin targets identified in the ProtoArray screen in the absence of Ca^{2+}. Targets in bold are identified in the absence of Ca^{2+} only.

Microfluidic device preparation

Microfluidic devices were cast in PDMS (Sylgard 184, Dow Corning, Onecall, UK) using standard soft lithography methods(2). The clear PDMS was coloured black by the addition of a small quantity of carbon nanopowder, 0.2% w/w, prior to curing (Sigma, UK). Inlet and outlet holes were punched using a biopsy punch (WPI, Florida, US). The PDMS devices were bonded to glass slides in a plasma oven using an oxygen plasma (Diener Electronics, Germany). The electrodes were fabricated by placing the bonded device glass slide down on a hot plate set to 79°C and inserting InBiSn alloy (51% In, 32.5% Bi, 16.5% Sn, Conro Electronics, UK) through the solder inlet, Fig. 1A. The electrodes were automatically aligned with the fluidic channel by an array of micropillars. These pillars defined the border between fluidic and solder channels, whilst maintaining direct contact between the liquid and the metal electrodes.

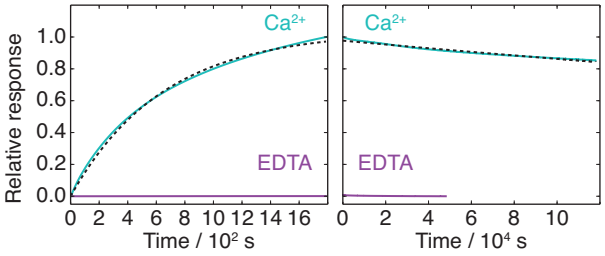

Figure 3: SPR measurements. Interaction between phosphorylase kinase and immobilised calmodulin. Left: association of phosphorylase kinase in the presence of Ca^{2+} in cyan, with the fit represented by the dashed line. The magenta line shows the signal in the presence of EDTA. No binding was detected in the absence of Ca^{2+}, the data in EDTA has therefore been normalised to the maximum signal in the calcium buffer. The dissociation data is shown in the right panel.

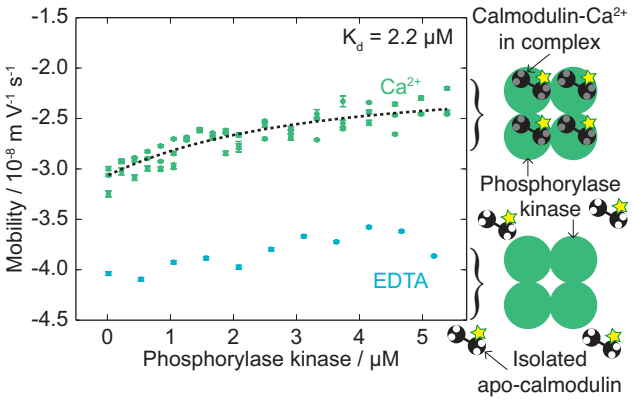

Figure 4: Calmodulin and phosphorylase kinase. (a) The observed electrophoretic mobility of calmodulin in response to an increasing concentration of phosphorylase kinase, in the presence of either 0.1 mM $CaCl_2$ (green) or 0.1 mM EDTA (blue).

Electrophoresis experiments

Electrophoresis experiments were performed in the type of microfluidic device seen in Fig. 1. Binding curves for calmodulin-target protein interactions were obtained by investigating samples containing a fixed concentration of Alexa488 labelled calmodulin and a varying concentration of target protein. The concentration ranges investigated were adjusted so as to reach a plateau in the observed electrophoretic mobility. In the case of phosphorylase kinase the solubility of the target protein was also a consideration.

Four repeats of a voltage range at set increments were performed for each protein concentration. Three images and current readings were obtained at each voltage step, Fig. 3. The voltage range and increments were adjusted to achieve considerable sample deflection, and thereby a relatively low error on δ, whilst avoiding the accumulation of electrolysis products at the electrode interfaces.

For a 1:1 interaction between calmodulin, C, and the target protein binding sites, P, with the total concentrations of C_t and P_t, K_d can be determined from the observed electrophoretic mobility, if there is a difference between the mobility of C and the complex, CP.

$$K_d = \frac{[\mathrm{C}] \cdot [\mathrm{P}]}{[\mathrm{CP}]} = \frac{[\mathrm{C}] \cdot (\mathrm{P_t} - \mathrm{C_t} + [\mathrm{C}])}{\mathrm{C_t} - [\mathrm{C}]}, \tag{4}$$

The observed electrophoretic mobility is the weighted sum of the fractional contributions from the mobilities of the isolated calmodulin, μ_c, and bound calmodulin, μ_{cp}

$$\mu_{obs} = \mu_c \frac{[\mathrm{C}]}{\mathrm{C_t}} + \mu_{\mathrm{cp}} \frac{[\mathrm{CP}]}{\mathrm{C_t}}, \tag{5}$$

the quadratic equation, Eqn. 6, was solved for [C].

$$0 = [\mathrm{C}]^2 + (K_d + \mathrm{P_t} - \mathrm{C_t}) \cdot [\mathrm{C}] - K_d \cdot \mathrm{C_t} \tag{6}$$

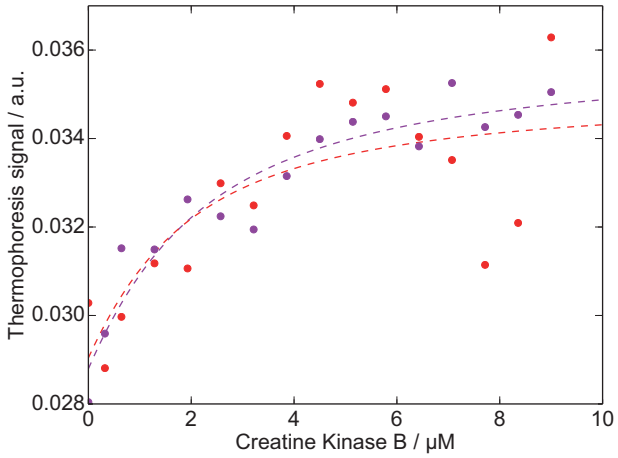

Figure 5: Thermophoresis experiments with calmodulin and creatine kinase B. The binding of 1 μM Alexa488-labelled calmodulin to creatine kinase B was monitored by thermophoresis. The experiments were carried out in a low ionic strength buffer: 0.1 mM $CaCl_2$, 5 mM Tris-HCl pH 8.0 (red) and in a high salt buffer: 150 mM KCl, 0.1 mM $CaCl_2$, 5 mM Tris-HCl pH 8.0 (magenta). Fits to the thermophoresis signal resulted in $K_d = 1.4$ μM for the low ionic strength buffer (red line) and $K_d = 1.7$ μM for the measurements at high salt concentrations (magenta line).

The resulting expression for [C] in terms of $\mathrm{P_t}$, $\mathrm{C_t}$, and K_d is shown below in equation 7.

$$[\mathrm{C}] = \mu_\mathrm{c} \frac{(-\mathrm{P_t} + \mathrm{C_t} - K_d + \sqrt{(\mathrm{P_t} - \mathrm{C_t} + K_d)^2 + 4K_d\mathrm{C_t}})}{2}. \tag{7}$$

By combining equations 7 and 5, we were able to fit the free flow electrophoresis data to obtain the equilibrium dissociation constants for the interactions investigated in this study. The two concentrations $[\mathrm{P_t}]$ and $[\mathrm{C_t}]$ were known experimental parameters, leaving μ_c μ_cp, and K_d as the fitting parameters.

Free flow electrophoresis with a known binding partner

In a set of positive control experiments, we evaluated the use of free flow electrophoresis to detect and characterise the binding of calmodulin to phosphorylase kinase, a well-documented ligand(3, 4). The activation of phosphorylase kinase in response to an increase in the intracellular Ca^{2+} concentration during muscle contraction leads to glycogenolysis(4–7). Phosphorylase kinase is a large, 1.3 MDa, hexadecameric complex, consisting of four repeats of its $\alpha\beta\gamma\delta$ subunits, each protein complex thus has four calmodulin binding sites. The δ subunit is an auto regulatory calmodulin homologue, it binds and activates the catalytic γ subunit in response to Ca^{2+}(3, 4).

We measured the electrophoretic mobilities of samples containing 1 μM calmodulin and 0 - 5.2 μM phosphorylase kinase $\alpha\beta\gamma\delta$ subunit in 5 mM Tris-HCl pH 8, 0.1 mM $CaCl_2$ by free flow electrophoresis, Fig. 4. In complementary experiments we also investigated the binding of 1 μM apo-calmodulin to phosphorylase kinase (0 to 5.0 μM $\alpha\beta\gamma\delta$) in 5 mM Tris-HCl pH 8 containing 0.1 mM EDTA to chelate any residual Ca^{2+}.

By measuring the change in electrophoretic mobility we were able to monitor the binding equilibrium between calmodulin and phosphorylase kinase in the presence of Ca^{2+}, green points in Fig. 4. In the absence of free Ca^{2+} we did not observe a monotonic change in the μ_obs for calmodulin, cyan points in Fig. 4, indicating a lack of interaction between the two proteins in the absence of free calcium ions. In agreement with the findings from the free flow electrophoresis experiments, when we performed SPR experiments investigating the binding of phosphorylase kinase to immobilised calmodulin, binding was only observed in the presence of free Ca^{2+}, see SI Fig. 3.

Thermophoresis

Thermophoresis experiments were conducted in 5 mM Tris-HCl pH 8.0, 0.1 mM $CaCl_2$ and either 0 mM or 150 mM KCl. Sixteen samples were prepared in each buffer with 1 μM Alexa488-calmodulin and creatine kinase B concentrations , $\mathrm{C_{CKB}}$

ranging from 0 to 9 μM, Fig. 5. The samples were placed in low-binding capillaries (MST Premium Coated from Nanotemper Technologies, Germany) and mounted in a Monolith NT.115 Instrument (Nanotemper Technologies, Germany) operated at 25°C. Thermophoresis measurements were performed using LED power 20% and themorophoresis 50% for 25 s. The thermophoresis signal, as a function of total creatine kinase B concentration, C, in μM, was fitted using a 1:1 binding equation:

$$\mathrm{Y} = \mathrm{Y}_{\mathrm{free}} + \mathrm{Y}_{\mathrm{bound}} \cdot \frac{\mathrm{X}}{\mathrm{X} + K_d} \tag{8}$$

where

$$\mathrm{X} = -0.5 \cdot (K_d + 1.0 - \mathrm{C}_{\mathrm{CKB}}) + \sqrt{0.25 \cdot (K_d + 1.0 - \mathrm{C}_{\mathrm{CKB}})^2 + \mathrm{C}_{\mathrm{CKB}} \cdot K_d} \tag{9}$$

where Y is calculated signal, $\mathrm{Y}_{\mathrm{free}}$ its contribution from free Alexa488-calmodulin and $\mathrm{Y}_{\mathrm{bound}}$ its contribution from Alexa488-calmodulin bound to creatine kinase B. X is the free creatine kinase B concentration, $\mathrm{C}_{\mathrm{CKB}}$ the total creatine kinase B concentration in μM, 1.0 is the total Alexa488-calmodulin concentration in μM. Fits to the thermophoresis signal resulted in K_d = 1.4 μM for the low ionic strength buffer and K_d = 1.7 μM for the measurements at high salt concentrations, see Fig. 5.

References

1. Waltersson, Y., S. Linse, P. Brodin, and T. Grundström, 1993. Mutational effects on the cooperativity of Ca2+ binding in calmodulin. Biochemistry 32:7866–7871.
2. McDonald, J. C., and G. M. Whitesides, 2002. Poly (dimethylsiloxane) as a material for fabricating microfluidic devices. Acc. Chem. Res. 35:491–499.
3. Cohen, P., A. Burchell, J. Foulkes, P. T. W. Cohen, T. C. Vanaman, and A. C. Nairn, 1978. Identification of the Ca2+-dependent modulator protein as the fourth subunit of rabbit skeletal muscle phosphorylase kinase. FEBS Lett. 92:287–293.
4. Cook, A. G., L. N. Johnson, and J. M. McDonnell, 2005. Structural characterization of Ca2+/CaM in complex with the phosphorylase kinase PhK5 peptide. FEBS J. 272:1511–1522.
5. Meyer, W. L., E. H. Fischer, and E. G. Krebs, 1964. Activation of Skeletal Muscle Phosphorylase b Kinase by CA2+ *. Biochemistry 3:1033–1039.
6. Brostrom, C. O., F. L. Hunkeler, and E. G. Krebs, 1971. The Regulation of Skeletal Muscle Phosphorylase Kinase by Ca2+. J. Biol. Chem. 246:1961–1967.
7. Priddy, T. S., C. R. Middaugh, and G. M. Carlson, 2007. Electrostatic changes in phosphorylase kinase induced by its obligatory allosteric activator Ca2+. Prot. Sci. 16:517–527.